Efficient Mercury(II) Capture by Functionalized Poly(pyrrole methane)s: the Role of Chloro and Imino Groups

Ziyu Guo[a], Zhenyu Wang[a], Jinbo Liu [a], Yaxing Sun [a], Liu Yang [a], Jiangtao Feng [a,c*], Bo Hou[b*], Wei Yan [a]

[a] Department of Environmental Engineering, Xi'an Key Laboratory of Solid Waste Recycling and Resource Recovery, School of Energy and Power Engineering, Xi'an Jiaotong University, Xi'an, 710049, China.

[b] School of Physics and Astronomy, Cardiff University, The Parade, Cardiff, CF24 3AA, UK

[c] Jiangsu Engineering Laboratory of New Materials for Sewage Treatment and Recycling, Soochow University, Suzhou, Jiangsu 215123, China

[*]Corresponding authors:

Jiangtao Feng: fjtes@xjtu.edu.cn; Bo Hou: HouB6@cardiff.ac.uk

Abstract: Efficient mercury ion removal from water is a primary challenge for ecosystem protection and public health. This study improves the effect of functional groups on mercury removal by functionalizing and tuning the molecular structure of poly(pyrrole ethene) (PPyE) with chloro, i.e. poly[pyrrole-2,5-bis(2-chloroethane)] (PPyCE), and imino groups, i.e. poly[pyrrole-2,5-bis(2-ethylamino ethane)] (PPyEE). The resultant functionalized poly(pyrrole methane)s can efficiently remove mercury (Hg(II)) from water with uptake capacities of 684.59 mg/g (chloro functionalized) and 389.57 mg/g (imino functionalized) at room temperature, which was much higher than that of unfunctionalized poly(pyrrole ethane) (only 122.74 mg/g). The functionalized poly(pyrrole methane)s had additional benefits of low usage, excellent selectivity for mercury ions and anti-coexisting ion interference performance. Furthermore, the chloro functionalized poly(pyrrole methane)s also exhibited exceptional recyclability for the adsorption capacity remaining above 90% of the original after 5 regeneration cycles. These results were largely attributed to the functional groups of chloro and imino in the material backbone as chelating sites to bind with mercury, which was confirmed by Fourier Transform infrared spectroscopy (FT-IR) and X-ray photoelectron spectroscopy (XPS) before and after mercury capture. This study provides a potential strategy for designing and tuning the adsorbents to efficiently remove mercury and other heavy metal ions from aqueous solutions for environmental remediation.

Key words: poly(pyrrole methane)s, adsorption, mercury, chloro-functinalization, imino-functionalization

1 Introduction

Mercury which exists in various chemical forms such as elemental mercury (Hg^0), methyl mercury (CH_3Hg^+), and inorganic mercury (Hg^{2+}) is a toxic heavy metal that circulates in the atmosphere, water and soil around the world. [1-3], which are mainly from coal combustion, papermaking, oil refining and electroplating, metallurgy, and battery manufacturing [1, 4]. Mercury (Hg) pollution has a severe threat to the ecosystem and further public health for invading the human body through the food chain. The World Health Organization (WTO) sets the upper limit of mercury content in drinking water and wastewater as 1 μg/L and 5 μg/L respectively to reduce the impact of mercury on the environment and human health [5, 6]. With the continuous development of global gold mining industry and fossil fuel burning, mercury pollution has a gradually increasing trend. Therefore, monitoring and controlling mercury pollution is imminent according to the Minamata Convention in 2017 [7]. In many environments affected by mercury contamination, water is an environment that cannot be ignored because it can act as a "storage closet" for mercury. It is imperative to develop effective technologies for the mercury pollution remediation in water.

Various technologies, such as chemical precipitation [8, 9], coagulation [10, 11], membrane separation [12], ion exchange [13, 14] and adsorption [15-18], have been developed for mercury removal from water. Among these methods, adsorption has been attractive for its advantages of high removal efficiency, environmental friendliness, and excellent operability, especially suitable for the treatment of low concentration pollution [19]. Various adsorbents have been used to remove mercury from water, including carbon materials [20-23], zeolite [24], mesoporous silica [25, 26], chitosan [27, 28], metal organic frameworks (MOFs) [29-33], MXenes [23, 34], other organic polymers [1, 35], and covalent organic frameworks (COFs) [36-38].

In recent years, conductive polymers, including polyaniline (PANI), polypyrrole (PPy), and polythiophene (PTh) have also been developed as a novel adsorbent that

effectively removes heavy metal ions from water [39-42]. Poly(pyrrole methane)s as a derivative of polypyrrole can be synthesized from pyrrole and aldehyde at acidic conditions, making it easy to introduce various functional groups with promising uptake capacities by changing the type of aldehyde. Functional groups (-COOH, -OH, -SH, -NH_2, etc.) exert a very important part in the adsorption of heavy metal ions in water [43-46]. For example, sPAN with sulfhydryl, carboxyl and amino groups experts a good performance for mercury removal which equilibrium adsorption amount could be as high as 459.3 (±16.0) mg/g[46]. Due to the special affinity between functional groups and heavy metal ions, some functional groups can enhance the adsorption capacity of the adsorbent and improve the adsorption selectivity at the same time. For instance, poly(pyrrole methane)s with aromatic groups can form three steric hindrance structures with distinct mercury-capture selectivity because of three different substitution sites on the benzene ring [47]. However, the influence of the interaction between different functional groups in poly(pyrrole methane)s and heavy metals on their adsorption capacity and selectivity is still a considerable of challenge.

Herein, we design and synthesis poly(pyrrole ethene) (PPyE), poly[pyrrole-2,5-bis(2-chloroethane)](PPyCE), poly[pyrrole-2,5-bis(2-ethylamino ethane)] (PPyEE) by chemical polymerization approach, which potentially can address the challenge of polymer adsorption capacity and selectivity on mercury removal. The as-prepared poly(pyrrole methane)s with chloro and imino groups feature highly accessible Hg(II) capture with a strong adsorption selectivity for mercury in the presence of other cations. Furthermore, the poly(pyrrole methane)s with chloro and imino groups have a highest saturation uptake capacity up to 836.47 mg/g for Hg(II) at 318 K and can be easily regenerated and recycled 5 cycles without significant loss of mercury uptake capacity. Moreover, chloro and imino groups in the poly(pyrrole methane) backbone are found to be the main binding sites to mercury ions, and chloro group display greater influence on the Hg(II) capture than that of imino group.

2 Materials and methods

2.1 Materials

Pyrrole (98%), acetaldehyde solution (40%), 2-chloroacetaldehyde solution (40%), ethylamine solution (65%~70%), dichloromethane, hydrochloric acid (HCl), sodium hydroxide (NaOH), nitric acid (HNO_3), thiourea, N,N-Dimethylformamide (DMF), $Hg(NO_3)_2·H_2O$, $Cd(NO_3)_2·H_2O$, $Cu(NO_3)_2·H_2O$, $Zn(NO_3)_2·H_2O$, $Pb(NO_3)_2·H_2O$, KNO_3, $Ca(NO_3)_2$, $Mg(NO_3)_2$, NaCl, Na_2SO_4 were bought from Sinopharm Chemical Reagent Co., Ltd. All reagents were of analytical grade and used as received. And we used the EPED-40TF Superpure Water System (EPED, Nanjing, China) to produce the deionized water used in this work.

2.2 Preparation of the poly(pyrrole methane)s

(1) Preparation of PPyE

The poly(pyrrole ethane) (PPyE) was synthesized as follows: Firstly, 3.5 mL (0.00035 mol) acetaldehyde solution was dissolved into 100 mL DMF and then 25 mL HCl (12 mol/L) was added .Finally, 1.4 mL (0.00014 mol) pyrrole was dissolved into 75mL DMF and added into the above solution to catalyze the polymerization. The mixture solution was stirred (300 rpm) at 333K for 24 h. After the reaction, the mixture was poured into 800 mL of 2% ammonia aqueous solution and obtained brownish solid precipitation. The solid was soaked in the ammonia solution for 2 h, then filtered and washed with lots of water until the filtrate is neutral. Finally, the obtained solid was Soxhlet extracted with ethanol for 24 hours, and then dried at 333K for 12 hours. The black solid powder was obtained and named PPyE.

(2) Preparation of PPyCE

The synthesis method of poly[pyrrole-2,5-bis(2-chloroethane)] (PPyCE) was the same as that of PPyE except for replacing 1.1 mL (0.02mol) acetaldehyde solution with 2-chloroacetaldehyde solution.

(3) Preparation of PPyEE

The poly[pyrrole-2,5-bis(2-ethylamino ethane)] (PPyEE) was synthesized as follows: 1.0 g of PPyCE was swollen in 5 ml of dichloromethane at 298K for 12 hours, Then the swollen PPyCE was transferred into 20 mL of ethylamine/ethanol (volume ratio: 1:1) at 323K for 12 h. Then we used the deionized water to wash the solid until the filtrate was neutral, after that, the solid was dried in an oven at 333K for 12 hours. The obtained black solid was named PPyEE [48].

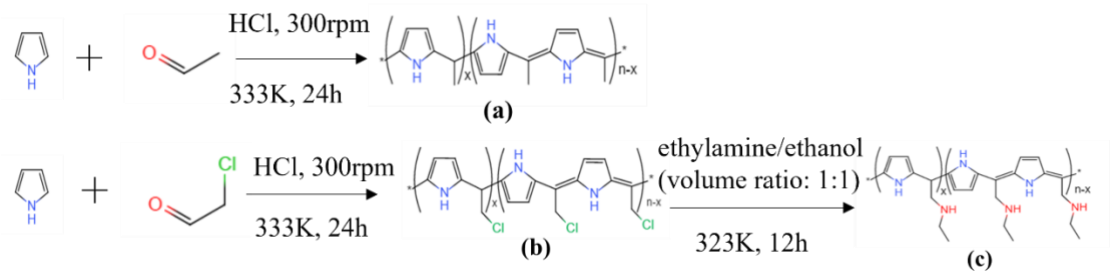

Scheme 1. Molecular structures of PPyE(a), PPyCE(b) and PPyEE(c).

2.3 Characterizations

The following tests and equipments were applied to characterize and test the three adsorbents, so as to clarify the structural properties and adsorption mechanism of the adsorbent. We used a FT-IR spectrophotometer (Bruker TENSOR 37, Switzerland) to scan the Fourier transform infrared (FT-IR) spectra in the region of 4000-400 cm^{-1} by the KBr pellet method. The morphology was examined by scanning electron microscope (SEM) with the energy dispersive X-ray spectrometry (EDX, Gemini 500, Zeiss, Germany) based on the secondary electron information generated under high vacuum and 10 kV voltage. We use physical adsorption device (SSA-4200, Beijing Builder Co. Ltd, China) to perform the Barrett-Emmett-Teller specific surface area (S_{BET}), average pore radius (R) and total pore volume (V) at 77 K. The Zeta potentials of the samples were measured by zeta potential and particle size analyzer (Brookhaven 90plus Zeta, U.S.) by adding 1 mg sample in 10 mL NaCl solution (10^{-3} $mol \cdot L^{-1}$) with different pH values (pH=1-12, adjusted by 1.0 $mol \cdot L^{-1}$ HNO_3 or NaOH solution). X-ray photoelectron spectroscopy (XPS) spectra were performed on a photoelectron

spectrometer (Kratos Axis Ultra DLD, Shimadzu, Japan) with an Al monochromatic X-ray source (1486.71 eV), and we used the C 1s hydrocarbon peak at 284.8 eV to revise all the binding energies (BEs). The concentration of heavy metal ions (Pb^{2+}, Cd^{2+}, Cu^{2+} and Zn^{2+}) was analyzed by the inductively coupled plasma optical emission spectrometer (ICP-OES, ICPE-9000, Japan). pH values of the solution were detected by a pH meter (FE28-Standard, Mettler Toledo)..

2.4 Batch adsorption experiments

In the adsorption experiment, all solutions containing cations are prepared from corresponding nitrates, and the solutions containing anions are corresponding to sodium. Prepare 1000 mg/L Hg(II) stock solution by dissolving analytical grade $Hg(NO_3)_2 \cdot H_2O$ in 0.2 mol/L HNO_3 solution. The simulated solution used in the subsequent experiments was prepared with deionized water to dilute the stock solution, and the pH value was adjusted with 0.1 mol/L HNO_3 or NaOH solution. Centrifuge tubes (50 mL) containing 4 mg adsorbent and 20 mL of 100 mg/L mercury ion solution was ultrasonically treated for 2 minutes to achieve uniform dispersion of the adsorbent in the liquid, and then transferred in a constant temperature shaker to adsorb at 200 rpm for 24 hours at 298 K. After the adsorption reaction, the solution was filtered by polyethersulfone membrane with the pore size of 0.45 μm. We did three groups of parallel samples and take the average value as the result. The concentration of mercury ion was tested by an inductively coupled plasma optical emission spectrometer (ICP-OES, ICPE-9000, Japan). The adsorption efficiency (η) and adsorption capacity at time t (q_t) were calculated from the following equations (Eqs. (1) and (2)).

$$\eta = \frac{C_0 - C_e}{C_0} \times 100\% \tag{1}$$

$$q_t = \left(\frac{C_0 - C_t}{m} \right) V \tag{2}$$

where q_t (mg/g) is the adsorption capacity of the adsorbent at time t, it can be as q_e if C_t is the adsorbate concentration at adsorption equilibrium. C_0 and C_t (mg/L) are

concentrations of heavy metal ions in solution at the initial and time *t*, respectively, *m* (g) is the adsorbent mass, and *V* (L) is the volume of solution.

For the kinetics study, 80 mg of poly(pyrrole methane)s was added into 400 mL of 100 mg/L Hg(II) solution at pH 5. The reaction system was stirred with magnetic stirring at a speed of 200 rpm and kept at 298 K with a water bath. At time zero and preselected time intervals (0-420 min), 2 mL samples were removed and quickly filtered through polyethersulfone membrane for Hg(II) concentration analysis.

To investigate the pH effect on Hg(II) removal by the as-prepared poly(pyrrole methane)s, the solution initial pH values were adjusted from 2 to 7 with 0.1 mol/L HNO_3 or NaOH solution. Different dosages are designed in the range of 0.1-0.5 g/L to study the effect of adsorbent dosage. In addition, adsorption isotherm studies were carried out by changing the initial concentration of Hg(II) from 10 to 200 mg/L at four different temperatures (288 K, 298 K, 308 K, 318 K).

The effect of background ions (Ca^{2+}, Mg^{2+}, K^{+}, SO_4^{2-}, Cl^{-}) was investigated in a binary adsorption mode, and the concentration of background ions was 10 mmol/L. Furthermore, in order to study the selective adsorption performance of the adsorbent, mixed solutions were explored. The competitive heavy metal ions included Pb (II), Cd (II), Cu (II) and Zn (II), with the same concentration of 100 mg/L of Hg (II).

The regeneration and reusability of poly(pyrrole methane)s were investigated by batch-cycle adsorption-desorption experiments. Typically, 20 mg of poly(pyrrole methane)s was added into 100 mL of Hg(II) solution (100 mg/L, pH=5-6). The exhausted poly(pyrrole methane)s were accomplished with 100 mL solution containing 0.1 mol/L HCl and 1 wt% thiourea and vibrating for 3 h at 298 K. The mixture was filtered, and the Hg (II) concentrations were analyzed. Then the adsorbent was washed with deionized water until the filtrate was neutral for the next adsorption-desorption cycle.

3 Results and Discussion

3.1 Characterization of the poly(pyrrole methane)s

Fig. 1 exhibits the FT-IR spectra of the as-prepared poly(pyrrole methane)s. The main feature bands could be assigned as follows: the peak at around 3426 cm^{-1} is the N-H stretch [47, 49], the weak characteristic peak at and 3000-2900 cm^{-1} is related to the C-H stretch of methyl, methylene and backbone of PPy [49], respectively. The peaks at 1628 and 1407 cm^{-1} were consistent with C=C stretching[50, 51] and C-N stretching of the pyrrole ring, respectively [52]. The peak at 940 cm^{-1} is ascribed to the stretching of C-Cl bond [53]. The broad adsorption band at 2100 cm^{-1}-2000 cm^{-1} in PPyEE is attributed to C-N stretching in ethylamine [54]. Compared with that of PPyCE, the peak intensity at 940 cm^{-1} of PPyEE is weaker, indicating the decline of the population of C-Cl bonds. But the peak at 940 cm^{-1} still exists in FT-IR spectrum of PPyEE, which illustrates that the C-Cl band has not completely replace by C-N in the structure of PPyEE which may be conducive to the adsorption of mercury ions. These peaks in the FT-IR spectra indicate that the PPyE, PPyCE and PPyEE are polymerized successfully.

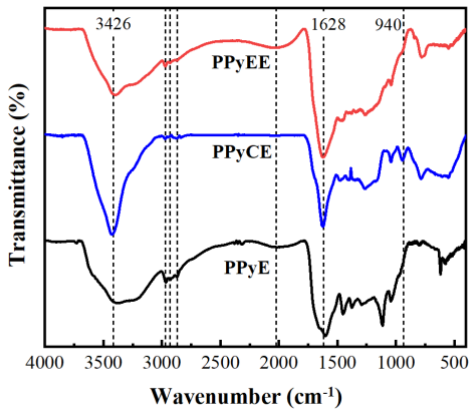

Fig.1. FT-IR spectra of the as-prepared poly(pyrrole methane)s.

The morphologies of the poly(pyrrole methane)s are characterized by SEM and shown in Fig.2. All samples show irregular granules shapes and the particle size ranges from 2 μm to 50 μm. Meanwhile, the particle size of PPyE and PPyEE is larger than that of PPyCE. The results of EDS (Fig.S1) show that PPyEE contains more N (11.31%)

but less Cl (0.81%) than that of PPyCE with 7.49% of N and 3.58% of Cl (Table 1), meaning that the PPyCE and PPyEE are polymerized successfully, which is consistent with the result of FT-IR.. The existence of oxygen may be due to the adsorbed water in the samples.

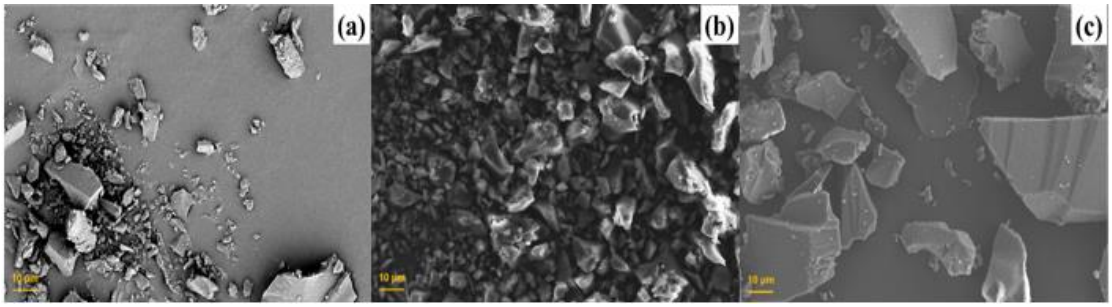

Fig.2. SEM images of PPyE(a), PPyCE (b) and PPyEE (c).

Table 1 Elements contents of the as-prepared poly(pyrrole methane)s from EDS test

Samples	C/ wt%	N/ wt%	O/ wt%	Cl/ wt%
PPyE	86.84	5.60	7.56	0
PPyCE	76.90	7.49	12.03	3.58
PPyEE	76.81	11.31	11.07	0.81

The nitrogen adsorption-desorption isotherm and pore size distribution of the three samples are tested (Fig. S2 and S3) and the textural properties of the samples are shown in Table 2. It can be seen that the S_{BET} and V of PPyCE could attain 22.11 m^2/g and 0.09 cm^3/g, which are much bigger than that of PPyE and PPyEE. Larger specific surface area may mean higher adsorption capacity. PPyCE with the largest specific surface area may have the largest adsorption capacity for mercury ions in the three poly(pyrrole methane)s.

Zeta potential can reflect the surface charge of adsorbent and influence the interactions between adsorbates and adsorbents. When the solution pH is lower than pH_{PZC}, the materials will be positively charged and when the solution pH is higher than the pH_{PZC}, the materials will be negatively charged. Fig.3 shows the zeta potentials of the three prepared poly(pyrrole methane)s at different pH. It can be seen that the pH_{PZC} values of PPyCE and PPyEE are both 4.81, and that of PPyE is 5.02 which is a little higher than that of PPyCE and PPyEE.

Table 2 Textural properties of the as-prepared poly(pyrrole methane)s

Samples	S_{BET} **(m^2/g)**	V **(cm^3/g)**	R **(nm)**

PPyE	2.33	0.014	3.1
PPyCE	22.11	0.090	2.4
PPyEE	2.23	0.012	3.1

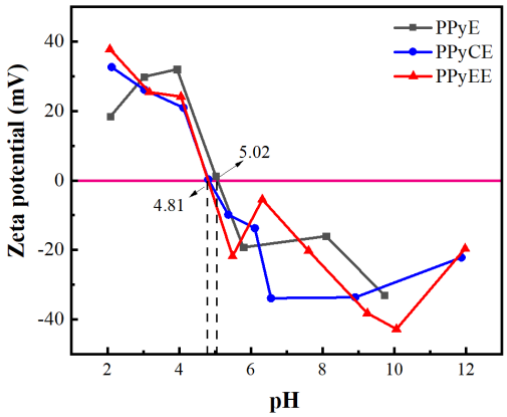

Fig.3 Zeta potentials of the as-prepared poly(pyrrole methane)s at different pH.

3.2 Investigation of adsorption properties

3.2.1 Effect of initial pH

The adsorption of heavy metal ions onto organic materials is greatly affected by the pH value of the solution. In this study, the adsorption capacity of Hg(II) onto poly(pyrrole methane)s at different pH (2-7) was studied ans shown in Fig. 4. It can be seen that the adsorption capacity of Hg(II) onto the as-prepared poly(pyrrole methane)s is highly pH-dependent, increasing with pH from 2 to 4, and then being a plateau at pH from 4 to 7. For mercury ions in water, $Hg(OH)^+$ and Hg^{2+} are the dominant species in the solution at pH of 2-3. At this pH, both the samples are positively charged as their pH_{PZC} was near 5 (Fig. 3), higher than solution pH. Therefore, the low mercury adsorption capacity at this pH may be attributed to electrostatic repulsion between the positively charged mercury and the adsorbent. With pH increase, mercury ions gradually convert to neutral $Hg(OH)_2(aq)$ and the zeta potential of the samples decline, which weakens the electrostatic repulsion. When pH is over 5, neutral $Hg(OH)_2(aq)$ is the dominant species, the electrostatic repulsion with the adsorbent is negligible. $Hg(OH)_2(aq)$ complexed with surface functional groups of the adsorbent may be preferred, which is consistent with the higher adsorption capacity at this pH range.[4].

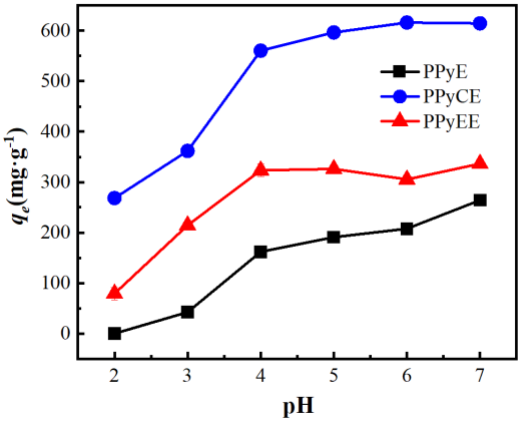

Fig. 4. Effect of solution pH on the adsorption of Hg(II) onto the poly(pyrrole methane)s. (a dosage of 0.4 g/L of PPyE, 0.2 g/L of PPyCE and 0.3 g/L PPyEE, C_0=100mg/L, T=298K)

3.2.2 Effect of dosage

The adsorption dosage is one of the most fundamental parameters for adsorption. Studying the suitable amount of adsorbent can provide economic reference for the practical application of adsorbent. The removal rate of Hg(II) by the as-prepared poly(pyrrole methane)s with different dosages is shown in Fig.5. We can see that with the increasing dosage, the removal rate increases rapidly which is attributed to the growing available adsorption sites with the increase of adsorbent. The maximum adsorption removal rate can be reached as the adsorbent dosage is at a low dosage of 0.2-0.4 g/L. At this time, the removal rate of mercury ions gradually reached 100% for PPyCE and 90% for PPyEE. Therefore, the dosage of 0.2 g/L of PPyCE, 0.3 g/L of PPyEE and 0.4 g/L PPyE were chosen in the following experiments.

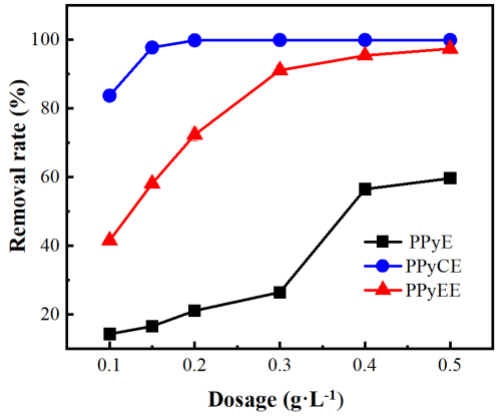

Fig. 5. Effect of dosage on the removal of Hg(II) by the poly(pyrrole methane)s(C_0=100mg/L,

pH= 5-6, T=298K)

3.2.3 Adsorption kinetics

The change of adsorption process with time can reflect the speed of adsorption process. The influence of the contact time for adsorption capacity of Hg(II) onto PPyE, PPyCE and PPyEE is shown in Fig.6. The adsorption of Hg(II) onto the as-prepared poly(pyrrole methane)s increased rapidly in the first 100 min and obviously slowed down due to the decrease of the adsorbent active sites. The adsorption gradually reaches equilibrium after about 200 min. PPyCE and PPyEE have lower dosage of 0.2g/L and 0.3g/L respectively, but as shown in Fig. 6 below, they have higher adsorption rate and adsorption capacity than PPyE.

Pseudo-first-order (PFO), pseudo-second-order (PSO) models and Elovich model were employed to fit the adsorption kinetic data of Hg(II) onto the as-prepared poly(pyrrole methane)s and their equations are given in Eqs. (3) (4) and (5) [55-58], respectively.

$$q_t = q_e(1-e^{-k_1 t}) \tag{3}$$

$$q_t = \frac{k_2 q_e^{\,2} t}{1+k_2 q_e t} \tag{4}$$

$$q_t = \frac{1}{\beta}\ln(1+\alpha\beta t) \tag{5}$$

where q_t (mg/g) is the amount adsorbed at time t (min), and q_e (mg/g) is the equilibrium adsorption capacity[59], k_1 (1/min) and k_2 (g/(mg·min)) are the rate constants for the pseudo-first-order and pseudo-second-order, respectively. α (mg/(g·min)) is the initial rate constant and β (mg/g) is the desorption constant.

Table 3 depicted the kinetic parameters for the three models. It can be seen that the correlation coefficients of the Elovich model (R^2 = 0.988 and 0.965) are more suitable for describing the adsorption kinetics of the ae-prepared poly(pyrrole methane)s for Hg(II) than PFO model (R^2 = 0.969 and 0.847) and PSO model (R^2 = 0.980 and 0.908), indicating the adsorption of Hg(II) onto poly(pyrrole methane)s

involved a chemical adsorption process. Moreover, the relatively bigger rate constant α (Elovich model) indicates that PPyEE has the higher initial adsorption rate than the others [55].

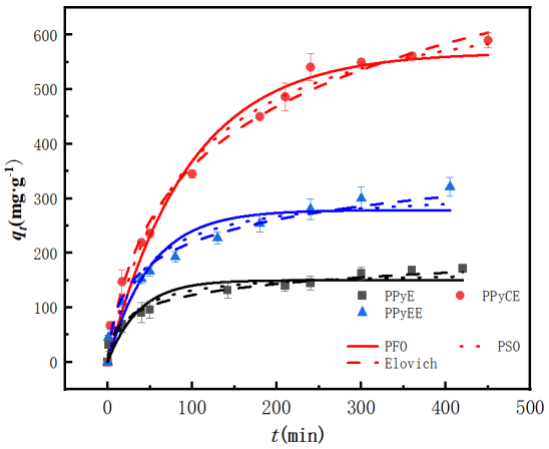

Fig. 6. Adsorption kinetics model of Hg(II) onto poly(pyrrole methane)s (a dosage of 0.4 g/L of PPyE, 0.2 g/L of PPyCE and 0.3 g/L PPyEE, C_0=110mg/L, pH= 5-6, T=298K)

Table 3 Kinetic parameters for Hg(II) adsorption by poly(pyrrole methane)s

Samples	PFO			PSO			Elovich		
	k_1 (1/min)	q_e (mg/g)	R^2	k_2 (g/(mg·min))	q_e (mg/g)	R^2	α (mg/(g min))	β (mg/g)	R^2
PPyE	0.027	150.09	0.892	0.00022	166.74	0.937	18.01	0.035	0.979
PPyCE	0.011	568.22	0.969	0.00016	699.93	0.980	11.78	0.006	0.988
PPyEE	0.020	278.54	0.847	0.00084	316.72	0.908	21.21	0.016	0.965

3.2.4 Adsorption isotherm

Adsorption isotherm exerts an important part to evaluate the adsorption capacities of adsorbents and investigate interactions between adsorbates and adsorbents. In this study, Langmuir and Freundlich isotherms were employed to analyze the adsorption data. Their non-linear formulas are expressed by Eqs. (6) and (7) [60, 61].

$$q_e = \frac{q_{max} K_L C_e}{1 + K_L C_e} \quad (6)$$

$$q_e = K_F C_e^{1/n} \quad (7)$$

where C_e (mg/L) is the equilibrium concentration; q_e (mg/g) is equilibrium adsorption capacity and q_{max} (mg/g) is the maximum adsorption capacity of adsorbents; K_L (L/mg)

is the Langmuir constant which is related to the affinity of adsorbate and the binding sites; K_F ((mg/g)/(mg/L)$^{1/n}$) is the Freundlich constant indicated the relative adsorption capacity of the adsorbents and n is a dimensionless constant related to the intensity of adsorption.

The adsorption isotherms of Hg(II) adsorbed onto poly(pyrrole methane)s at different temperatures are shown in Fig. 7 and the relevant parameters are listed in Table 4. For the three poly(pyrrole methane)s, R^2 values of the Langmuir model are a little higher than that of the Freundlich model, indicating their adsorption process was a monolayer adsorption. Moreover, as the temperature increased from 288 K to 318 K, the maximum adsorption capacities (q_{max}) of Hg(II) onto PPyE, PPyCE and PPyEE, calculated from Langmuir model increase from 95.02 to 239.55 mg/g, 636.73 to 836.47 mg/g and from 288.08 to 539.65 mg/g, respectively. The endothermic property of the adsorption process may be due to the increase in the thermal energy of the adsorbing species with increasing temperature [62, 63]. Meanwhile, the adsorption isotherm results illustrate that the modification of poly(pyrrole methane)s by chloro and imino groups can dramatically improve its adsorption capacity for Hg(II).

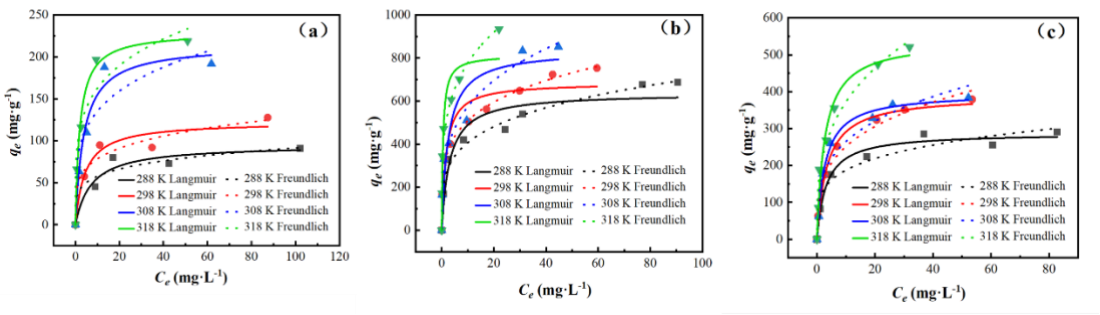

Fig. 7. Adsorption isotherm for the adsorption of Hg(II) onto PPyE(a), PPyCE(b) and PPyEE(c)(a dosage of 0.4 g/L of PPyE, 0.2 g/L of PPyCE and 0.3 g/L PPyEE, C_0=100mg/L, pH= 5-6, T= 298K~318K)

Table 4 Langmuir and Freundlich isotherm parameters for Hg(II) adsorption by poly(pyrrole methane)s

Samples	T	Langmuir model			Freundlich model		
		q_{max}	K_L	R^2	n	K_F	R^2
PPyE	288	95.02	0.14	0.924	5.02	36.48	0.901
	298	122.74	0.23	0.935	4.68	48.01	0.945
	308	229.16	0.26	0.965	4.23	78.55	0.861
	318	239.55	0.50	0.986	4.50	97.45	0.917

PPyCE	288	636.73	0.33	0.923	4.14	233.17	0.983
	298	684.59	0.63	0.899	4.45	303.65	0.996
	308	813.66	0.41	0.880	3.61	303.15	0.984
	318	836.47	2.02	0.924	4.12	444.13	0.983
PPyEE	288	288.08	0.32	0.979	4.47	111.87	0.943
	298	389.57	0.29	0.991	3.55	131.48	0.973
	308	396.29	0.37	0.992	3.66	141.16	0.931
	318	539.65	0.38	0.971	3.15	179.21	0.966

3.2.5 Thermodynamic parameters

Thermodynamic parameters, such as enthalpy change (ΔH, kJ/mol), entropy change (ΔS, kJ/(mol·K)) and the free energy change (ΔG, kJ/mol), can reflect the spontaneous degree of adsorption process and can be derived based on Eqs. (8-9) [64, 65].

$$\Delta G = -RT\ln K_d \quad (8)$$

$$\Delta G = \Delta H - T\Delta S \quad (9)$$

where K_d=q_e/C_e(L/g) is the adsorption equilibrium constant; R (8.314 J/(mol·K)) is the universal gas constant, and T (K) is the absolute temperature.

The changes of ΔG with temperature T are shown in Fig. S4, and the obtained values of ΔG, ΔH and ΔS under different temperatures were listed in Table 5. The negative values of ΔG and positive ΔH indicate that the Hg(II) adsorption process was spontaneous and endothermic [63]. The positive values of ΔS reveals that the randomness of the solid liquid interface may increase when Hg(II) is adsorbed onto poly(pyrrole methane)s [47]. Moreover, the ΔG values decreased with the increase in temperature, which suggested that spontaneity increase with increasing temperature.

Table 5 Thermodynamic parameters for Hg(II) adsorption by poly(pyrrole methane)s.

Samples	ΔG(KJ/mol)				ΔH(KJ/mol)	ΔS (KJ/(mol·K))
	288 K	298 K	308 K	318 K		
PPyE	-0.27	-0.94	-2.90	-3.85	41.58	0.14
PPyCE	-4.85	-6.29	-7.55	-9.91	42.65	0.16
PPyEE	-3.01	-4.85	-5.11	-7.38	35.45	0.13

3.2.6 Effect of the co-existing ions on Hg(II) adsorption

In addition to heavy metal ions, K^+, Ca^{2+}, Mg^{2+}, Cl^-, SO_4^{2-} as background ions widely existed in various water bodies, which may have impact on the adsorption process of heavy metals. Therefore, it is necessary to study the effect of background ions on the adsorption process. The effect of background ions (including K^+, Ca^{2+}, Mg^{2+}, Cl^-, SO_4^{2-}) on the removal of Hg(II) byPPyE, PPyCE and PPyEE was studied and the results are presented in Fig. 8a. As can be seen from Fig. 8a, the background ions such as K^+, Ca^{2+}, Mg^{2+}, and SO_4^{2-} have no obvious impact on Hg(II) adsorption, but Cl^- has strong inhibitory effect. The existence of Cl^- reduced the removal rates of mercury ions by PPyE, PPyCE and PPyEE to 17.29%, 38.8% and 51.07%, respectively. This is because the presence of 10 mmol/L NaCl complicates the formation of mercury species. According to previous works, under the condition of pH = 5-6, Cl^- and Hg(II) formed multiple complexes, in which $HgCl_2$ was the dominant species, reaching around 90%, $HgCl_3^-$accounted for nearly 10%, and a small amount of HgClOH, which are not easy to complex with adsorbents compared with $Hg(OH)_2$[66] .

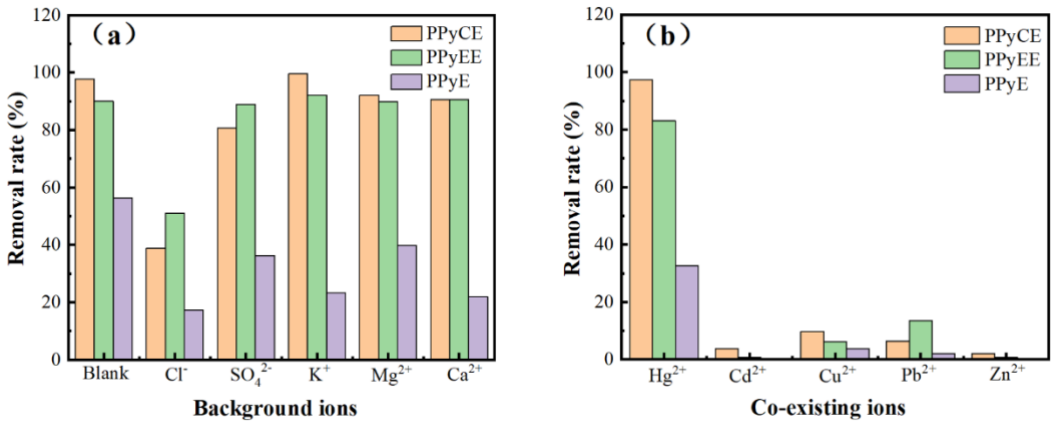

Fig. 8. Effect of background ions (a) and co-existing heavy metal ions (b) on the removal of Hg(II) by poly(pyrrole methane)s. (a dosage of 0.4 g/L of PPyE, 0.2 g/L of PPyCE and 0.3 g/L PPyEE, C_0=100mg/L, pH= 5-6, T=298K)

Furthermore, several co-existing heavy metal ions may influence the adsorption of Hg(II) from water. For the application of adsorbent, selective adsorption is one of the most important aspects. It can be seen from Fig. 8b that the removal rates of mercury

ions by PPyE, PPyCE and PPyEE were 65.65%, 97.28% and 83.01%, respectively, while the removal rates of the co-existing heavy metal ions (such as Cd^{2+}, Cu^{2+}, Pb^{2+} and Zn^{2+}) are basically below 10%, which indicates the exceptional adsorption selectivity of PPyCE and PPyEE for mercury ions and co-existing metal ions had no significant influence on the adsorption. These results indicate that PPyCE and PPyEE have much stronger affinity to Hg(II) than PPyE.

Distribution coefficients (K_d, L/g) and selectivity coefficient (α) were employed to study the degree of affinity and selectivity of materials. The large values of K_d indicate the metal ions can be commendably removed by poly(pyrrole methane)s, while large values of α indicate the better affinity and selectivity of poly(pyrrole methane)s for Hg(II) than other heavy metal ions. K_d and α could be extracted from Eqs. (10) and (11) [67, 68].

$$K_d = \frac{Q_e}{C_e} \tag{10}$$

$$\alpha = \frac{K_d(Hg)}{K_d(M_i)} \tag{11}$$

where $K_d(Hg)$ represented the distribution coefficients of Hg(II) and $K_d(M_i)$ was the distribution coefficients of co-existing heavy metal ions.

As can be seen from Table 6, the K_d value of Hg(II) is greater than that of the co-existing heavy metal ions, which indicates that the adsorption affinity between poly(pyrrole methane)s and Hg(II) is the largest.

In addition, the values of α for Cd and Zn are much bigger than that of Cu and Pb, indicates the poly(pyrrole methane)s have better selective adsorption performance in solutions containing Cd(II) and Zn(II) than that in solutions containing Cu and Pb. Meanwhile, PPyCE and PPyEE have bigger α values than that of PPyE, indicating the functionalization by chloro and imino groups improves the selective adsorption performance of poly(pyrrole methane)s for Hg(II). However, α values of PPyCE is bigger than that of PPyEE, which indicates that the functionalization with chloro group

can improve the selective adsorption performance of poly(pyrrole methane)s for Hg(II) more than that of functionalization with imino group.

Table 5 The K_d and α of heavy metal adsorption by the three poly(pyrrole methane)s

Metal ions	PPyE		PPyCE		PPyEE	
	K_d (L/g)	α	K_d (L/g)	α	K_d (L/g)	α
Hg	2.42	—	178.98	—	24.43	—
Cu	0.20	12.29	0.54	330.13	0.32	75.24
Pb	0.11	22.16	0.34	528.77	0.78	31.42
Cd	0.02	126.04	0.20	915.80	0.04	676.63
Zn	0.015	164.27	0.11	1691.40	0.03	762.13

3.2.7 Regeneration of PPyCE and PPyEE

The regeneration performance of an adsorbent is an important parameter to assess its practical application. In many reports, mixed solutions of acid and thiourea have been used to achieve effective desorption of mercury. On the one hand, thiourea, as a small molecule substance rich in sulfur and nitrogen, has a very strong binding ability with mercury[46, 69]. On the other hand, desorption is a reverse process of adsorption, and conditions unfavorable to adsorption must be favorable conditions for desorption. In our study, lower pH and Cl^- effectively inhibit the adsorption of mercury, so batch regeneration studies were carried out using the mixed solution of 0.1 mol/L HCl and 1.0 % thiourea as the desorption agent. Regeneration efficiency of the three as-prepared poly(pyrrole methane)s was evaluated by 5 consecutive cycles of adsorption-desorption experiments. (Fig. 9). The result shows that after five adsorption-desorption cycles, all poly(pyrrole methane)s can maintain more than 80% of the original adsorption capacity, indicating that the as-prepared poly(pyrrole methane)s have excellent adsorption stability for mercury ions.

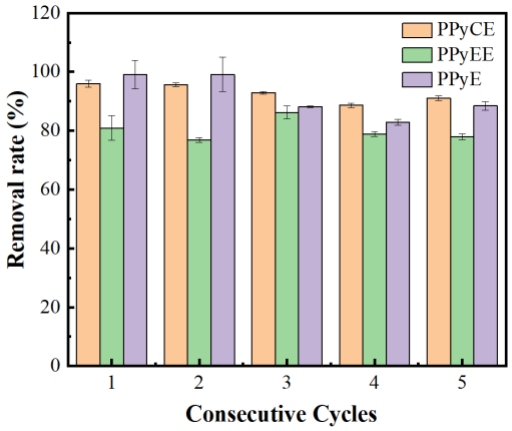

Fig. 9. Adsorption-desorption consecutive cycles of Hg(II) onto poly(pyrrole methane)s. (a dosage of 0.4 g/L of PPyE, 0.2 g/L of PPyCE and 0.3 g/L PPyEE, C_0=100mg/L, pH= 5-6, T=298K)

3.3 Adsorption Mechanism

To research the adsorption mechanism of the Hg(II) onto the functionalized poly(pyrrole methane)s, FT-IR and XPS test were applied to investigate the role of chloro and imino groups in the adsorption process.

FT-IR spectra of the functionalized poly(pyrrole methane)s before and after adsorption is shown in Fig. 10. It can be seen that the intensity of N-H stretching at around 3400 cm^{-1} after Hg(II) adsorption declines significantly compared with the peaks 1628 cm^{-1} which is ascribed to C=C stretching, indicating that the interaction between Hg(II) and imino group in PPyE, PpyCE and PpyEE. Meanwhile, the peak intensity of C-Cl stretching at 940 cm^{-1} is significantly weakened in the spectra of PPyCE after adsorption, which means the Cl active sites in PPyCE also play an important role in Hg(II) adsorption process. While in the spectra of PPyE and PPyEE, the intensity of the peak at around 1385 cm^{-1}, which is attributed to N-O stretching of NO_3^- [70, 71], are also sharply appeared after Hg(II) adsorption. This is mainly because of the proton acid doping process and NO_3^- for the adsorption solution is make up with $Hg(NO_3)_2$ as an electrically neutralizing ion binding to the molecular backbones of PPyEE [72]. FT-IR results indicate that the adsorption sites for Hg(II) removal occurred

at C-Cl and C-N-H positions in PPyCE and PPyEE molecular structure and at C-N-H position in PPyE.

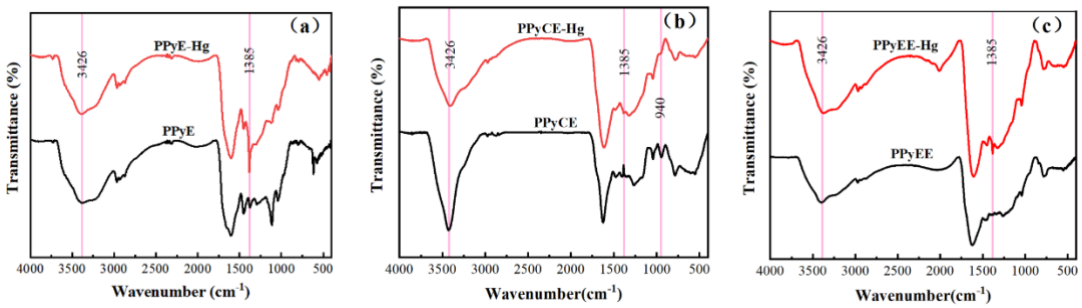

Fig.10. FT-IR spectra comparation of PPyE(a), PPyCE(b), PPyEE(c) before and after Hg(II) adsorption.

In order to further explore the role of chloro and imino groups in Hg(II) adsorption, XPS test was applied to give insight into the change of binding energy of the N1s, Cl 2p and Hg4f from the functional poly(pyrrole methane)s before and after Hg(II) adsorption. The intensity and position of C 1s have no obvious change before and after adsorption (Fig. S5 a-c), indicating that Hg(II) adsorption has not occurred in the groups associated with carbon. In the full-scan spectrum (Fig. 11a-c), the new binding energy peaks (Hg 4f) are observed after Hg(II) absorption. The binding energy of Hg 4f could be split two different peaks at 104.9-105.5 eV and 100.9-101.5 eV, which illustrates that Hg(II) have been successfully adsorbed by the as-prepared poly(pyrrole methane)s (Fig. S5 d-f). EDS results after Hg(II) adsorption are consistent with XPS results (Fig S6).

The binding energy peak of N 1s can be divided into three peaks from Fig. 11 d-f. The three fitting peaks, centered at about 397.3 eV, 399.7-399.8 eV, and 402.2-402.7 eV respectively, are ascribed to pyridinic N, pyrrolic N, and oxidized N, respectively [73-75]. After Hg(II) adsorption, the ratio of the three types of nitrogen changes, which indicates that the electron transfer occurs during the adsorption, indicating that the forms of nitrogen converted to each other in Hg(II) adsorption process [76]. These results indicate that nitrogen atoms involved in the adsorption process of Hg(II) onto PPyE, PPyCE and PPyEE. Meanwhile, the position change of binding energy for the three types of nitrogen also proves the positive role of imino group in Hg(II) adsorption.

Fig. 11g-h is the high resolution of Cl 2p peak of PPyCE and PPyEE before and after Hg(II) adsorption. The peak at 196.4-198.4 eV is attributed to ionic chlorine (Cl^-), and the peak at 199.8-200.1 eV correspond to Cl in C-Cl groups [77, 78]. Additionally, the relative intensity of C-Cl declined significantly, while the position of ionic chlorine peak has shifted evidently after Hg(II) adsorption, which illustrates C-Cl group can be consider as one of the important active chemisorbed sites (forming $HgCl_2$)to remove Hg(II) from water [47, 79].

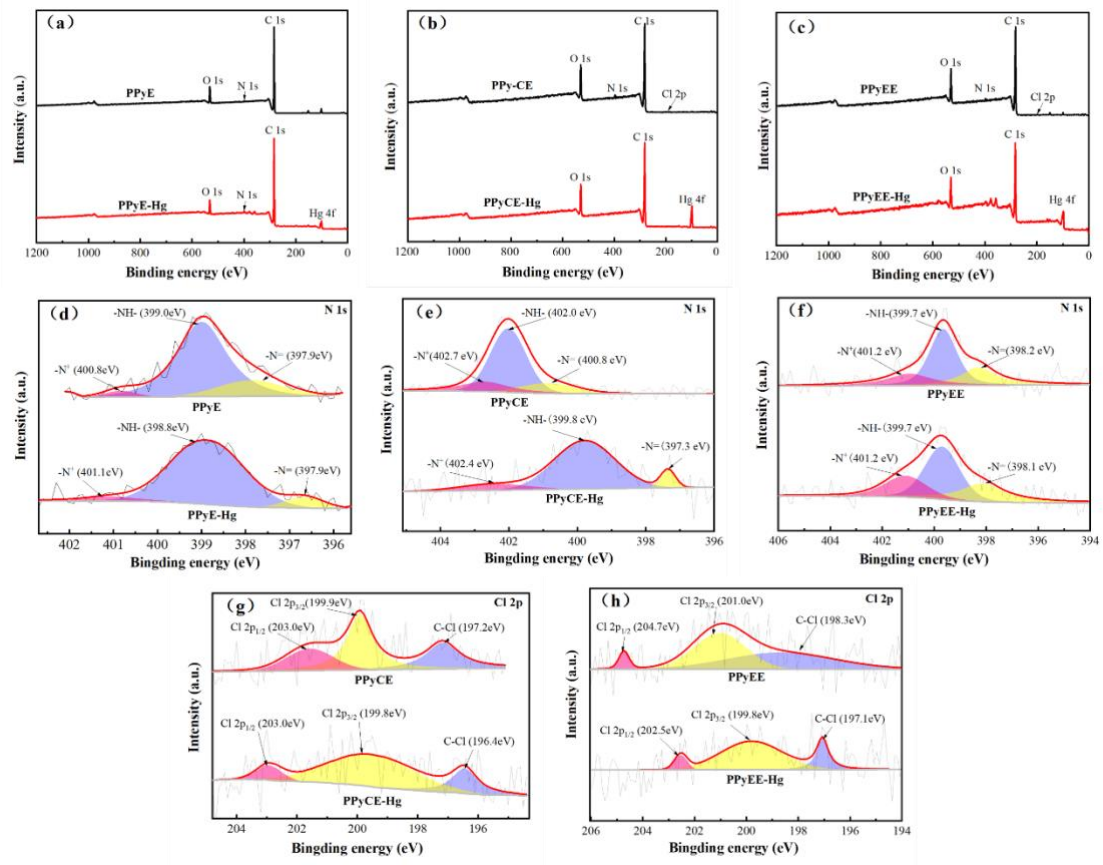

Fig.11. Full scan survey XPS spectra of PPyE(a), PPyCE(b), PPyEE(c) and high resolution spectra of (d-f) N 1 s, (g-h) Cl 2p of PPyE, PPyCE, PPyEE before and after Hg(II) adsorption.

4 Conclusion

In this research, the effect of cholro or imino groups on the adsorption of mercury ions onto poly(pyrromethene)s was explored. Cholro and imino functionalized poly(pyrromethene)s possessed high Hg(II) uptake capacities of 684.59 mg/g (PPyCE) and 389.57 mg/g (PPyEE) at room temperature and have additional benefits of low

dosage of 0.2 g/L forvPPyCE and 0.3 g/L for PPyEE, respectively. The cholro and imino functionalized poly(pyrromethene)s were also good recyclable with maintaining more than 80% of the original adsorption capacity after 5 cycles, and highly selective for Hg(II) in the presence of other cations. Efficient mercury removal was rapid due to the strong interaction between chlorine and imino groups and mercury ions. These results not only explore the effect of chlorine and imino groups on the adsorption of mercury ions, but also demonstrate the feasibility of poly(pyrromethene)s as adsorbent materials for heavy metal capture in wastewater remediation application.

Declaration of Competing Interest

The authors declare that they have no known competing financial interests or personal relationships that could have appeared to influence the work reported in this paper.

Acknowledgement

Jiangtao Feng acknowledges the National Natural Science Foundation of China (No. 52070155 and No. 51978569) and the Open Project of Jiangsu Engineering Laboratory of New Materials for Sewage Treatment and Recycling (No. SDGC2127). Bo Hou acknowledges the support from the Cardiff University, and Royal Society of Chemistry (No. E21-9668828170). The authors also acknowledge the financial support from the IEC\NSFC\211201-International Exchanges 2021 Cost Share (NSFC) and the Instrumental Analysis Center of Xi'an Jiaotong University for the help in SEM, XPS test and analysis.

Fundings

This project was financially supported by the National Natural Science Foundation of China (No. 52070155 and No. 51978569), the Open Project of Jiangsu Engineering Laboratory of New Materials for Sewage Treatment and Recycling (No. SDGC2127), the Cardiff University, and Royal Society of Chemistry (No. E21-9668828170) and the financial support from the IEC\NSFC\211201-International Exchanges 2021 Cost Share (NSFC).

References

[1] N. Ballav, R. Das, S. Giri, A.M. Muliwa, K. Pillay, A. Maity, L-cysteine doped polypyrrole (PPy@ L-Cyst): A super adsorbent for the rapid removal of Hg+2 and efficient catalytic activity of the spent adsorbent for reuse, Chem. Eng. J. 345 (2018) 621-630.

[2] F. Luo, J.L. Chen, L.L. Dang, W.N. Zhou, H.L. Lin, J.Q. Li, S.J. Liu, M.B. Luo, High-performance Hg2+ removal from ultra-low-concentration aqueous solution using both acylamide- and hydroxyl-functionalized metal-organic framework, J. Mater. Chem. A 3 (2015) 9616-9620.

[3] P. Holmes, K.A.F. James, L.S. Levy, Is low-level environmental mercury exposure of concern to human health?, Sci. Total Environ. 408 (2009) 171-182.

[4] X. Dong, L.Q. Ma, Y. Zhu, Y. Li, B. Gu, Mechanistic Investigation of Mercury Sorption by Brazilian Pepper Biochars of Different Pyrolytic Temperatures Based on X-ray Photoelectron Spectroscopy and Flow Calorimetry, Environ. Sci. Technol. 47 (2013) 12156-12164.

[5] X. Yan, P. Li, X. Song, J. Li, B. Ren, S. Gao, R. Cao, Recent progress in the removal of mercury ions from water based MOFs materials, Coord. Chem. Rev. 443 (2021).

[6] F.J. Alguacil, F.A. Lopez, Adsorption Processing for the Removal of Toxic Hg(II) from Liquid Effluents: Advances in the 2019 Year, Met. 10 (2020).

[7] Y. Fu, Y. Sun, Z. Chen, S. Ying, J. Wang, J. Hu, Functionalized magnetic mesoporous silica/poly(m-aminothiophenol) nanocomposite for Hg(II) rapid uptake and high catalytic activity of spent Hg(II) adsorbent, Sci. Total Environ. 691 (2019) 664-674.

[8] J.-H. Richard, C. Bischoff, C.G.M. Ahrens, H. Biester, Mercury (II) reduction and co-precipitation of metallic mercury on hydrous ferric oxide in contaminated

groundwater, Sci. Total Environ. 539 (2016) 36-44.
[9] T.A. Saleh, Experimental and analytical methods for testing inhibitors and fluids in water-based drilling environments, Trac-Trends in Analytical Chemistry 149 (2022).
[10] S.M. Bachand, T.E.C. Kraus, D. Stern, Y.L. Liang, W.R. Horwath, P.A.M. Bachand, Aluminum- and iron-based coagulation for in-situ removal of dissolved organic carbon, disinfection byproducts, mercury and other constituents from agricultural drain water, Ecol. Eng. 134 (2019) 26-38.
[11] Y.K. Henneberry, T.E.C. Kraus, J.A. Fleck, D.P. Krabbenhoft, P.M. Bachand, W.R. Horwath, Removal of inorganic mercury and methylmercury from surface waters following coagulation of dissolved organic matter with metal-based salts, Sci. Total Environ. 409 (2011) 631-637.
[12] I. Zawierucha, A. Nowik-Zajac, J. Lagiewka, G. Malina, Separation of Mercury(II) from Industrial Wastewater through Polymer Inclusion Membranes with Calix 4 pyrrole Derivative, Membr. 12 (2022).
[13] A. Oehmen, D. Vergel, J. Fradinho, M.A.M. Reis, J.G. Crespo, S. Velizarov, Mercury removal from water streams through the ion exchange membrane bioreactor concept, J. Hazard. Mater. 264 (2014) 65-70.
[14] C. Hernandez-Tamargo, B. Kwakye-Awuah, A.J. O'Malley, N.H. de Leeuw, Mercury exchange in zeolites Na-A and Na-Y studied by classical molecular dynamics simulations and ion exchange experiments, Microporous Mesoporous Mater. 315 (2021).
[15] L. Huang, R. Shen, R. Liu, Q. Shuai, Thiol-functionalized magnetic covalent organic frameworks by a cutting strategy for efficient removal of Hg2+ from water, J. Hazard. Mater. 392 (2020).
[16] E.V. Liakos, M. Mone, D.A. Lambropoulou, D.N. Bikiaris, G.Z. Kyzas, Adsorption Evaluation for the Removal of Nickel, Mercury, and Barium Ions from Single-Component and Mixtures of Aqueous Solutions by Using an Optimized Biobased Chitosan Derivative, Polym. 13 (2021).
[17] M. Al-Yaari, T.A. Saleh, Mercury Removal from Water Using a Novel Composite of Polyacrylate-Modified Carbon, Acs Omega 7 (2022) 14820-14831.
[18] M. Al-Yaari, T.A. Saleh, O. Saber, Removal of mercury from polluted water by a novel composite of polymer carbon nanofiber: kinetic, isotherm, and thermodynamic studies, RSC Adv. 11 (2021) 380-389.
[19] T. Kegl, A. Kosak, A. Lobnik, Z. Novak, A.K. Kralj, I. Ban, Adsorption of rare earth metals from wastewater by nanomaterials: A review, J. Hazard. Mater. 386 (2020).
[20] L. Wang, D. Hou, Y. Cao, Y.S. Ok, F.M.G. Tack, J. Rinklebe, D. O'Connor, Remediation of mercury contaminated soil, water, and air: A review of emerging materials and innovative technologies, Environ. Int. 134 (2020).105281
[21] P. Hadi, M.-H. To, C.-W. Hui, C.S.K. Lin, G. McKay, Aqueous mercury adsorption by activated carbons, Water Res. 73 (2015) 37-55.

[22] T.A. Saleh, Carbon nanotube-incorporated alumina as a support for MoNi catalysts for the efficient hydrodesulfurization of thiophenes, Chem. Eng. J. 404 (2021).
[23] T.A. Saleh, Global trends in technologies and nanomaterials for removal of sulfur organic compounds: Clean energy and green environment, J. Mol. Liq. 359 (2022).
[24] H. Shirzadi, A. Nezamzadeh-Ejhieh, An efficient modified zeolite for simultaneous removal of Pb(II) and Hg(II) from aqueous solution, J. Mol. Liq. 230 (2017) 221-229.
[25] P. Figueira, M.A.O. Lourenco, E. Pereira, J.R.B. Gomes, P. Ferreira, C.B. Lopes, Periodic mesoporous organosilica with low thiol density - a safer material to trap Hg(II) from water, J. Environ. Chem. Eng. 5 (2017) 5043-5053.
[26] T.A. Saleh, Protocols for synthesis of nanomaterials, polymers, and green materials as adsorbents for water treatment technologies, Environmental Technology & Innovation 24 (2021).
[27] H. Zeng, L. Wang, D. Zhang, P. Yan, J. Nie, V.K. Sharma, C. Wang, Highly efficient and selective removal of mercury ions using hyperbranched polyethylenimine functionalized carboxymethyl chitosan composite adsorbent, Chem. Eng. J. 358 (2019) 253-263.
[28] M. Sun, G. Cheng, X. Ge, M. Chen, C. Wang, L. Lou, X. Xu, Aqueous Hg(II) immobilization by chitosan stabilized magnetic iron sulfide nanoparticles, Sci. Total Environ. 621 (2018) 1074-1083.
[29] M. Zhao, Z. Huang, S. Wang, L. Zhang, Y. Zhou, Design of L-Cysteine Functionalized UiO-66 MOFs for Selective Adsorption of Hg(II) in Aqueous Medium, ACS Appl. Mater. Interfaces 11 (2019) 46973-46983.
[30] M. Feng, P. Zhang, H.-C. Zhou, V.K. Sharma, Water-stable metal-organic frameworks for aqueous removal of heavy metals and radionuclides: A review, Chemosphere. 209 (2018) 783-800.
[31] L. Huang, M. He, B. Chen, B. Hu, A mercapto functionalized magnetic Zr-MOF by solvent-assisted ligand exchange for Hg2+ removal from water, J. Mater. Chem. A 4 (2016) 5159-5166.
[32] T.A. Saleh, Nanomaterials: Classification, properties, and environmental toxicities, Environmental Technology & Innovation 20 (2020).
[33] T.A. Saleh, Nanomaterials and hybrid nanocomposites for CO2 capture and utilization: environmental and energy sustainability, RSC Adv. 12 (2022) 23869-23888.
[34] X. Gao, Y. Zhou, Y. Tan, Z. Cheng, B. Yang, Y. Ma, Z. Shen, J. Jia, Exploring adsorption behavior and oxidation mechanism of mercury on monolayer Ti2CO2 (MXenes) from first principles, Appl. Surf. Sci. 464 (2019) 53-60.
[35] M. Karmakar, H. Mondal, M. Mahapatra, P.K. Chattopadhyay, S. Chatterjee, N.R. Singha, Pectin-grafted terpolymer superadsorbent via N-H activated strategic protrusion of monomer for removals of Cd(II), Hg(II), and Pb(II), Carbohydr. Polym. 206 (2019) 778-791.
[36] N. Huang, L. Zhai, H. Xu, D. Jiang, Stable Covalent Organic Frameworks for

Exceptional Mercury Removal from Aqueous Solutions, J. Am. Chem. Soc. 139 (2017) 2428-2434.

[37] P. Pei, Y. Xu, L. Wang, X. Liang, Y. Sun, Thiol-functionalized montmorillonite prepared by one-step mechanochemical grafting and its adsorption performance for mercury and methylmercury, Sci. Total Environ. 806 (2022).

[38] T.A. Saleh, G. Fadillah, E. Ciptawati, M. Khaled, Analytical methods for mercury speciation, detection, and measurement in water, oil, and gas, Trac-Trends in Analytical Chemistry 132 (2020).

[39] J. Chen, L. Zhang, J. Zhu, N. Wang, J. Feng, W. Yan, Adsorption of polythiophene/TiO2 composite for Zn (II), Pb (II) and Cu (II): Selectivity and synergistic effect investigation, Appl. Surf. Sci. 459 (2018) 318-326.

[40] J. Chen, J. Zhu, N. Wang, J. Feng, W. Yan, Hydrophilic polythiophene/SiO2 composite for adsorption engineering: Green synthesis in aqueous medium and its synergistic and specific adsorption for heavy metals from wastewater, Chem. Eng. J. 360 (2019) 1486-1497.

[41] H. Hajjaoui, A. Soufi, W. Boumya, M. Abdennouri, N. Barka, Polyaniline/Nanomaterial Composites for the Removal of Heavy Metals by Adsorption: A Review, J. Compos. Sci. 5 (2021).

[42] J. Chen, M. Yu, C. Wang, J. Feng, W. Yan, Insight into the Synergistic Effect on Selective Adsorption for Heavy Metal Ions by a Polypyrrole/TiO2 Composite, Langmuir 34 (2018) 10187-10196.

[43] B. Aguila, Q. Sun, J.A. Perman, L.D. Earl, C.W. Abney, R. Elzein, R. Schlaf, S. Ma, Efficient Mercury Capture Using Functionalized Porous Organic Polymer, Adv. Mater. 29 (2017).

[44] L. Fu, S. Wang, G. Lin, L. Zhang, Q. Liu, J. Fang, C. Wei, G. Liu, Post-functionalization of UiO-66-NH2 by 2,5-Dimercapto-1,3,4-thiadiazole for the high efficient removal of Hg(II) in water, J. Hazard. Mater. 368 (2019) 42-51.

[45] S.-Y. Ding, M. Dong, Y.-W. Wang, Y.-T. Chen, H.-Z. Wang, C.-Y. Su, W. Wang, Thioether-Based Fluorescent Covalent Organic Framework for Selective Detection and Facile Removal of Mercury(II), J. Am. Chem. Soc. 138 (2016) 3031-3037.

[46] W. Duan, J. Wang, L. Chang, L. Zhao, Z. Tian, Z. Huang, W. Huang, Adsorption of mercury(II) from water by a novel sPAN fiber containing sulfhydryl, carboxyl and amino groups, RSC Adv. 8 (2018) 38259-38269.

[47] Y. Liu, W. Zhang, C. Zhao, H. Wang, J. Chen, L. Yang, J. Feng, W. Yan, Study on the synthesis of poly(pyrrole methane)s with the hydroxyl in different substituent position and their selective adsorption for Pb2+, Chem. Eng. J. 361 (2019) 528-537.

[48] D. Chen, H. Yu, M. Pan, B. Pan, Hydrogen bonding-orientated selectivity of phosphate adsorption by imine-functionalized adsorbent, Chem. Eng. J. 433 (2022).

[49] T. Fu, Y. Niu, Y. Zhou, K. Wang, Q. Mu, R. Qu, H. Chen, B. Yuan, H. Yang, Adsorption of Mn(II) from aqueous solution by silica-gel supported polyamidoamine dendrimers: Experimental and DFT study, J. Taiwan Inst. Chem. Eng. 97 (2019) 189-

199.
[50] T.A. Saleh, Simultaneous adsorptive desulfurization of diesel fuel over bimetallic nanoparticles loaded on activated carbon, J. Cleaner Prod. 172 (2018) 2123-2132.
[51] T.A. Saleh, The influence of treatment temperature on the acidity of MWCNT oxidized by HNO3 or a mixture of HNO3/H2SO4, Appl. Surf. Sci. 257 (2011) 7746-7751.
[52] B. Li, M. Shi, D. Yan, M. Bai, Synthesis and photophysical characterization of MWCNTs/poly(pyrrolyl methine) composite with large third-order optical nonlinearity, Chem. Phys. Lett. 662 (2016) 280-285.
[53] H. Javadian, F.Z. Sorkhrodi, B.B. Koutenaei, Experimental investigation on enhancing aqueous cadmium removal via nanostructure composite of modified hexagonal type mesoporous silica with polyaniline/polypyrrole nanoparticles, J. Ind. Eng. Chem. 20 (2014) 3678-3688.
[54] B. Bouchet-Fabre, K. Zellama, C. Godet, D. Ballutaud, T. Minea, Comparative study of the structure of a-CNx and a-CNx : H films using NEXAFS, XPS and FT-IR analysis, Thin Solid Films 482 (2005) 156-166.
[55] B. Dou, V. Dupont, W. Pan, B. Chen, Removal of aqueous toxic Hg(II) by synthesized TiO2 nanoparticles and TiO2/montmorillonite, Chem. Eng. J. 166 (2011) 631-638.
[56] Y.-S. Ho, Review of second-order models for adsorption systems, J. Hazard. Mater. 136 (2006) 681-689.
[57] Y.S. Ho, Citation review of Lagergren kinetic rate equation on adsorption reactions, Scientometrics 59 (2004) 171-177.
[58] R. Soury, M. Jabli, T.A. Saleh, W.S. Abdul-Hassan, E. Saint-Aman, F. Loiseau, C. Philouze, H. Nasri, Tetrakis(ethyl-4(4-butyryl) oxyphenyl) porphyrinato zinc complexes with 4,4 '-bpyridin: synthesis, characterization, and its catalytic degradation of Calmagite, RSC Adv. 8 (2018) 20143-20156.
[59] T.A. Saleh, Isotherm, kinetic, and thermodynamic studies on Hg(II) adsorption from aqueous solution by silica- multiwall carbon nanotubes, Environmental Science and Pollution Research 22 (2015) 16721-16731.
[60] P. Baskaralingam, M. Pulikesi, V. Ramamurthi, S. Sivanesan, Equilibrium studies for the adsorption of acid dye onto modified hectorite, J. Hazard. Mater. 136 (2006) 989-992.
[61] J. Feng, Y. Liu, L. Zhang, J. Zhu, J. Chen, H. Xu, H. Yang, W. Yan, Effects of calcination temperature on organic functional groups of TiO2 and the adsorption performance of the TiO2 for methylene blue, Sep. Sci. Technol. 55 (2020) 672-683.
[62] M. Bhaumik, S. Agarwal, V.K. Gupta, A. Maity, Enhanced removal of Cr(VI) from aqueous solutions using polypyrrole wrapped oxidized MWCNTs nanocomposites adsorbent, J. Colloid Interface Sci. 470 (2016) 257-267.
[63] Y. Xu, J. Chen, R. Chen, P. Yu, S. Guo, X. Wang, Adsorption and reduction of chromium(VI) from aqueous solution using polypyrrole/calcium rectorite composite

adsorbent, Water Res. 160 (2019) 148-157.
[64] Q. Wang, Q. Dang, C. Liu, X. Wang, B. Li, Q. Xu, H. Liu, X. Ji, B. Zhang, D. Cha, Novel amidinothiourea-modified chitosan microparticles for selective removal of Hg(II) in solution, Carbohydr. Polym. 269 (2021).
[65] X. Zhao, G. Zhang, Q. Jia, C. Zhao, W. Zhou, W. Li, Adsorption of Cu(II), Pb(II), Co(II), Ni(II), and Cd(II) from aqueous solution by poly(aryl ether ketone) containing pendant carboxyl groups (PEK-L): Equilibrium, kinetics, and thermodynamics, Chem. Eng. J. 171 (2011) 152-158.
[66] J. Lv, L. Luo, J. Zhang, P. Christie, S. Zhang, Adsorption of mercury on lignin: Combined surface complexation modeling and X-ray absorption spectroscopy studies, Environ. Pollut. 162 (2012) 255-261.
[67] X. Wang, L. Yang, J. Zhang, C. Wang, Q. Li, Preparation and characterization of chitosan-poly(vinyl alcohol)/bentonite nanocomposites for adsorption of Hg(II) ions, Chem. Eng. J. 251 (2014) 404-412.
[68] G. Lin, T. Hu, S. Wang, T. Xie, L. Zhang, S. Cheng, L. Fu, C. Xiong, Selective removal behavior and mechanism of trace Hg(II) using modified corn husk leaves, Chemosphere. 225 (2019) 65-72.
[69] K. Fu, X. Liu, C. Lv, J. Luo, M. Sun, S. Luo, J.C. Crittenden, Superselective Hg(II) Removal from Water Using a Thiol-Laced MOF-Based Sponge Monolith: Performance and Mechanism, Environ. Sci. Technol. 56 (2022) 2677-2688.
[70] S.K. Verma, M.K. Deb, Nondestructive and rapid determination of nitrate in soil, dry deposits and aerosol samples using KBr-matrix with diffuse reflectance Fourier transform infrared spectroscopy (DRIFTS), Anal. Chim. Acta 582 (2007) 382-389.
[71] S. Katayama, N. Yamada, M. Awano, Preparation of silicate foams using HSi(OC2H5)(3) and their NOx adsorption behavior, J. Eur. Ceram. Soc. 24 (2004) 1957-1960.
[72] T. Raudsepp, M. Marandi, T. Tamm, V. Sammelselg, J. Tamm, Influence of ion-exchange on the electrochemical properties of polypyrrole films, Electrochim. Acta 122 (2014) 79-86.
[73] M. Zhou, X. Xie, Q. Liu, M. Zhang, C. Peng, F. Li, Q. Liu, Y. Song, J. Wu, Z. Qiao, Spherical In2S3 anchored on g-C3N4 nanosheets for efficient elemental mercury removal in the wide temperature range, Chem. Eng. J. 430 (2022).
[74] Y. Liu, N. Zhang, X. Liu, C. Chen, L.-Z. Fan, L. Jiao, Red phosphorus nanoparticles embedded in porous N-doped carbon nanofibers as high-performance anode for sodium-ion batteries, Energy Storage Mater. 9 (2017) 170-178.
[75] Y. Liu, N. Zhang, C. Yu, L. Jiao, J. Chen, MnFe2O4@C Nanofibers as High-Performance Anode for Sodium-Ion Batteries, Nano Lett. 16 (2016) 3321-3328.
[76] H. Liu, W. Ruan, Z. Zhang, F. Shen, Y. Zhou, H. Yang, Dual 2-dimensional CuSe/g-C3N4 nano-heterostructure for boosting immobilization of elemental mercury in flue gas, Chem. Eng. J. 435 (2022).
[77] G. Li, S. Wang, F. Wang, Q. Wu, Y. Tang, B. Shen, Role of inherent active constituents on mercury adsorption capacity of chars from four solid wastes, Chem.

Eng. J. 307 (2017) 544-552.
[78] H. Chen, L. Tang, Y. Hu, Y. Geng, L. Meng, W. Li, Z. Wang, Z. Li, Z. Huo, Investigating the pathways of enhanced Pb immobilization by chlorine-loaded biochar, J. Cleaner Prod. 344 (2022).
[79] A.R. Altaf, Y.G. Adewuyi, H. Teng, L. Gang, F. Abid, Elemental mercury (Hg-0) removal from coal syngas using magnetic tea-biochar: Experimental and theoretical insights, J. Environ. Sci. 122 (2022) 150-161.